Z. Geomorph. N. F.	53	1	23–45	Berlin · Stuttgart	March 2009

Decadal-scale analysis of ground movements in old landslides in western Belgium

by

Olivier Dewitte, Miet Van Den Eeckhaut,
Jean Poesen, and Alain Demoulin

with 9 figures and 1 table

Summary. More than 150 large deep-seated landslides have been mapped in the Flemish Ardennes. Slope instabilities that have occurred in this hilly area of western Belgium during the last decades correspond to ground movements within these pre-existing landslides. In order to identify the mechanisms and controlling factors of these ground movements, a good knowledge of their spatial and temporal distribution is critical. 13 landslides affecting two hills were investigated based on several DTMs extracted by aerial stereophotogrammetry and spanning the 1952–1996 period. Vertical ground displacements were measured at each pixel by DTM subtraction with a confidence value of ± 0.70 m. Horizontal displacements were also estimated within the landslides and along the head scarps through topographical profiles. Most observed movements displayed patterns typical of rotational landslides. Vertical and horizontal displacements vary in magnitude both spatially and temporally, with respective ranges −7.4 m–+3.8 m and 0–14 m. Many displacements are materialized in the field. We distinguished two kinds of slope processes, corresponding to either reactivation at a deeper level or shallower motion. The former re-uses pre-exiting surfaces of rupture located at depths of ~ 15–20 m and is associated with the largest subsidence and uplift. They are also smaller reactivations confined at the landslide head. The other displacements consist in (1) earth flows occurring in the zone of accumulation sometimes as a consequence of large upslope reactivations, and (2) small failures occurring randomly. While most movements were triggered by intense rainfall, their spatial and temporal distribution is strongly related with the nature of the vegetation cover and the human activity.

1 *Introduction*

Landsliding recently damaged building and other infrastructures in the Flemish Ardennes, western Belgium (fig. 1A), and it is now well established that most of these slope instabilities correspond to ground movements within pre-existing landslides (Ost et al. 2003, Dewitte et al. 2005, 2006, 2008, Van Den Eeckhaut 2006, Van Den Eeckhaut et al. 2007a). More than 150 old deep-seated landslides with a shear surface deeper than 3 m and a mean area of ~ 4 ha were reported in this hilly region through field survey and interpretation of aerial photographs and hillshade maps (Van Den Eeckhaut et al. 2005, 2007b). Based on interviews and analysis of written documents, the historical catalogue compiled by Van Den Eeckhaut (2006) revealed

DOI: 10.1127/0372-8854/2009/0053-0023 0372-8854/09/0023 $ 5.75

that most since 100 years correspond to landslide reactivation. They are divided into reactivations either limited to the main scarp or affecting the whole landslide. Other displacements correspond to shallow earth slides in the zone of accumulation. However, the catalogue mainly includes displacements easily identified in the field and on the aerial photographs (i. e., the largest and/or the most recent displacements) and/or movements that caused damages to infrastructures and that were reported in written documents. Therefore, slower, smaller and/or older movements as well as displacements occurring in less exposed parts of the region (e. g., the forested areas) were not necessarily considered in the catalogue. According to field observation of tilted trees and electricity poles, and hummocky topographies, it is actually obvious that more ground movements have affected many landslides over the last decades.

A clear understanding of the mechanisms and the controlling factors (i. e., predisposing, preparatory, and triggering factors) behind all these slope processes is thus critical for mitigating damages in this area. The factors controlling the landslide reactivation are similar to those controlling first-time landslide initiation. For example, reactivations can be triggered by earthquakes (Keefer 1984, Parise & Wasowski 1999, Jibson et al. 2000, Refice et al. 2002, Agnesi et al. 2005) and/or intense rainfall (Wasowski 1998, Parise & Wasowski 1999, Polemio & Sdao 1999, Fiorillo 2003, Demoulin & Glade 2004, Stefanini 2004, Cubito et al. 2005, Demoulin 2006, Lourenço et al. 2006). In some cases, reactivations result also from human activities like, for example, land use and land cover changes (Jakob 2000, Montgomery et al. 2000, Guthrie 2002, Glade 2003, Nyssen et al. 2003, Sidle et al. 2006, Van Den Eeckhaut et al. 2007a), and building operations (e. g. excavation and overloading) (Bentley & Siddle 1996, Cubito et al. 2005).

The purpose of this study is to better understand the current activity of the landslides in the Flemish Ardennes. We more specifically investigate the mechanisms and controlling factors of movements that have occurred for several decades within representative landslides. Based on accurate multi-temporal digital terrain models (DTMs), we map first the areas of ground movement, then we analyse their spatial and temporal distribution as well as the magnitude of the vertical and horizontal ground displacements. After field validation of the detected movements, we finally discuss their controlling factors.

2 *Study area*

The hilly region of the Flemish Ardennes (fig. 1A) was shaped by post-Diestian erosion affecting subhorizontal (dip of 4 m km^{-1} to the NNE) loose Tertiary marine sediments composed of almost impermeable clay layers alternating with more permeable clayey sand and sand layers (De Moor & Pissart 1992, Jacobs et al. 1999), which are overlain by Quaternary loess of varying thickness (Gullentops et al. 2001). The alternation of more permeable and almost impermeable layers favours the build-up of perched water tables and, where they rise to the ground surface, springs occur. Altitudes range between 10 m a. s. l. in the valley of the river Scheldt and 150 m a. s. l on the Tertiary ridges to the south (fig. 1A). The hillslope gradients are generally below 0.10 %. Valley asymmetry, with the steepest slopes generally facing south to northwest, is also observed. The topography, lithology and hydrology directly affect the land use and land cover of the Flemish Ardennes. Forests generally extend over the

steepest slopes and the tops to the south, whereon the loess cover is the thinnest. Pastures are mainly located on gentle and moderate slopes and in places too humid for crops whereas cultivation extends frequently on the flat tops of the lowest hills, notably close to the town of Oudenaarde, and on the hillslope foots, where loess deposits are thick. The region has a maritime temperate climate with an average annual temperature of ~ 10 °C and a mean annual rainfall of 800 mm distributed over all seasons.

As already suggested for other deep-seated landslides in eastern Belgium (Demoulin et al. 2003), the origin of the landslides of the Flemish Ardennes might lie in a combination of a seismic event and a period of heavy rainfall (Ost et al. 2003, Van Den Eeckhaut et al. 2007c). According to the Keefer's relation between maximum distance of landslides from fault and Richter magnitude ML (Keefer 1984), Van Den Eeckhaut (2006) estimated magnitudes between 5 and 6 to trigger landslides in the Flemish Ardennes. However, the biggest earthquake recorded in Belgium during the 20th century occurred within the Flemish Ardennes in June 1938 and, despite a magnitude ML of 5.6, no landslide was reported.

No new deep-seated landslide has developed for decades and because no written document describing a landslide initiation is found (Van Den Eeckhaut 2006), they are all assumed to be older than 100 years old. AMS radiocarbon dating of one landslide gave a minimum age of 8,700 BP, suggesting that some of them could have been initiated during the early Holocene, or even earlier under periglacial conditions (Van Den Eeckhaut et al. 2007c). In addition, witness to several reactivations that occurred within this landslide was also borne by carbon dating. Van Den Eeckhaut (2006) indicates that within ~ 15 % of these landslides one or several reactivations occurred over the last two decades. This is obviously linked to the reduced strength of the slipped material and the presence of shear surfaces. Moreover, the reactivations were often related to human intervention, such as drainage and land use changes. They generally occurred after wet periods with a monthly rainfall exceeding 100 mm and a 12-month antecedent rainfall depth exceeding 1,000 mm.

Field observations of recent reactivations and the analysis of the surface of rupture of several landslides by means of electrical resistivity measurements (Van Den Eeckhaut et al. 2007c) and DTMs analysis (Dewitte and Demoulin 2005, Dewitte et al. 2008) suggest that most of the landslides correspond to retrogressive, multiple rotational earth slides.

For this study, landslides were investigated on two hills culminating at altitudes between 75 and 85 m a. s. l. situated along the river Scheldt close to the town of Oudenaarde (fig. 1). The Leupegem hill, to the north, is affected by 3 landslides, and 10 landslides are developed on the Rotelenberg hill, to the south (fig. 1B). These landslides have a mean size of ~ 6 ha, a length of ~ 320 m, and a width of ~ 175 m, and their ~ 8-m-high main scarp delimits the abrupt fringe of the plateaus. They developed on slopes of 13–20 %, preferentially oriented to the W and N. Through morphometric measurements, the mean depth of the surface of rupture has been estimated in the range 15–40 m, implying displaced volumes of ~ 700,000 m^3 (Dewitte & Demoulin 2005). These values however correspond to a maximum estimation as demonstrated for landslide 1 (fig. 1B) by the analysis of its surface of rupture by multi-temporal DTM comparison and the analysis of slope profiles (Dewitte et al. 2008). From the morphological point of view, the selected landslides are representative of the Flemish Ardennes (Ost et al. 2003).

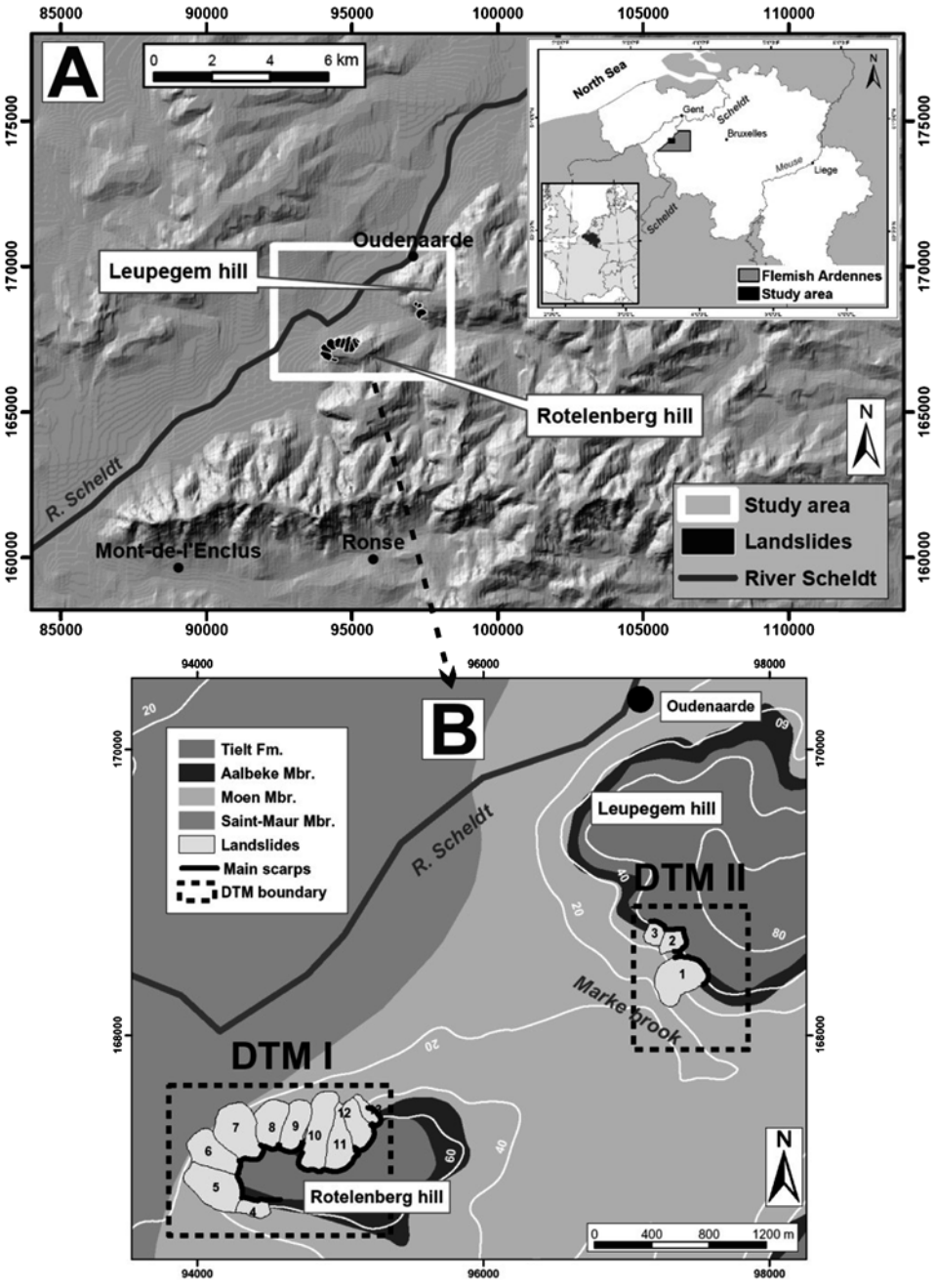
A
0 2 4 6 km
North Sea
Gent
Scheldt
Bruxelles
Meuse
Liege
Flemish Ardennes
Study area
Oudenaarde
Leupegem hill
Rotelenberg hill
R. Scheldt
Mont-de-l'Enclus
Ronse
Study area
Landslides
River Scheldt
B
Tielt Fm.
Aalbeke Mbr.
Moen Mbr.
Saint-Maur Mbr.
Landslides
Main scarps
DTM boundary
DTM I
DTM II
Marke brook
0 400 800 1200 m

The landslides are carved into subhorizontal Eocene sediments (fig. 1B). The three oldest Members belong to the Kortrijk Formation (Jacobs et al. 1999). At its base, the Saint-Maur Member (KoSm) is characterized by silty clays with a mean thickness of 27 m. Above, the Moen Member (KoMo), made of clayey coarse grey silt to fine sand with clay layers, may be up to 45 m thick. The overlying Aalbeke Member (KoAa) is a 10 m-thick layer composed of homogenous blue massive clays containing more than 50 % of clay minerals (Van Den Eeckhaut 2006). This Member is overlain by the Tielt Formation, which consists of micaceaous and glauconitic clayey sands alternating with clay layers and sandstone layers. The Aalbeke clays have been recognized as the layer most prone to landsliding, frequently causing the build-up of a perched water table and the occurrence of springs and swampy areas. The 13 main scarps are all in contact with, or just above the Aalbeke clays (fig. 1B).

The landslides under study are mainly covered by forests (mainly beech and poplar trees), pastures and cultivations (fig. 2), with a very small area covered by buildings (Dewitte 2006), the land use percentages being constant during the 44-year period of investigation (between 1952 and 1996) (fig. 2A). The landslides themselves are mainly covered by pastures and forests, while their main scarps are almost completely forested (except for landslides 3, 4, and 10). Forest dominates within landslides 7, 8, 9, 11, 12 and 13, while pasture extends almost exclusively at the foot of landslides 9 and 10 (Dewitte 2006). Cultivation predominates upslope of the landslide crowns, with limited change over time (fig. 2A).

Nevertheless, a more detailed analysis of the aerial photographs (fig. 2B) shows subtle but significant changes. Dewitte (2006) reported an increase in the size of the agricultural parcels for the whole study area, easily observed, e. g., on the plateau upslope of landslide 1 (fig. 2B). As exemplified for landslides 6 and 7, the forest appearance of the Rotelenberg hill changed, seeming more destructured in 1952, maybe due to selective timber harvesting. Except for its wooded foot, the land cover of landslide 1 was also modified. The area downslope of the main scarp, cultivated in 1952, was completely destructured in 1996 after a large reactivation in February 1995 (Van Den Eeckhaut et al. 2007a). Wooded in 1952, the main scarp of landslide 1 was completely unvegetated in 1996.

Fig. 1. Location of the study area. (A) Shaded LIDAR-derived map of the Flemish Ardennes showing the hilly morphology of the study area (DEM of Flanders acquired in 2002 and published in 2005 by OC GIS-Vlaanderen [MVG,-LIN-AWZ and MVG-LIN-ANIMAL]). The hillshade map was created with a light source azimuth of 135°, a light source elevation angle of 45° and a Z-factor of 5. The landslides (in black, with white boundaries) correspond to the mass movements investigated in this research. (B) Geological setting of the two hills of the study area. The scars and the main scarps of the 13 landslides are superposed on the Eocene lithologies. The quadrangles DTM I and DTM II locate the two DTMs used in the ground displacement analysis. The altitudes (in white) are in meters.

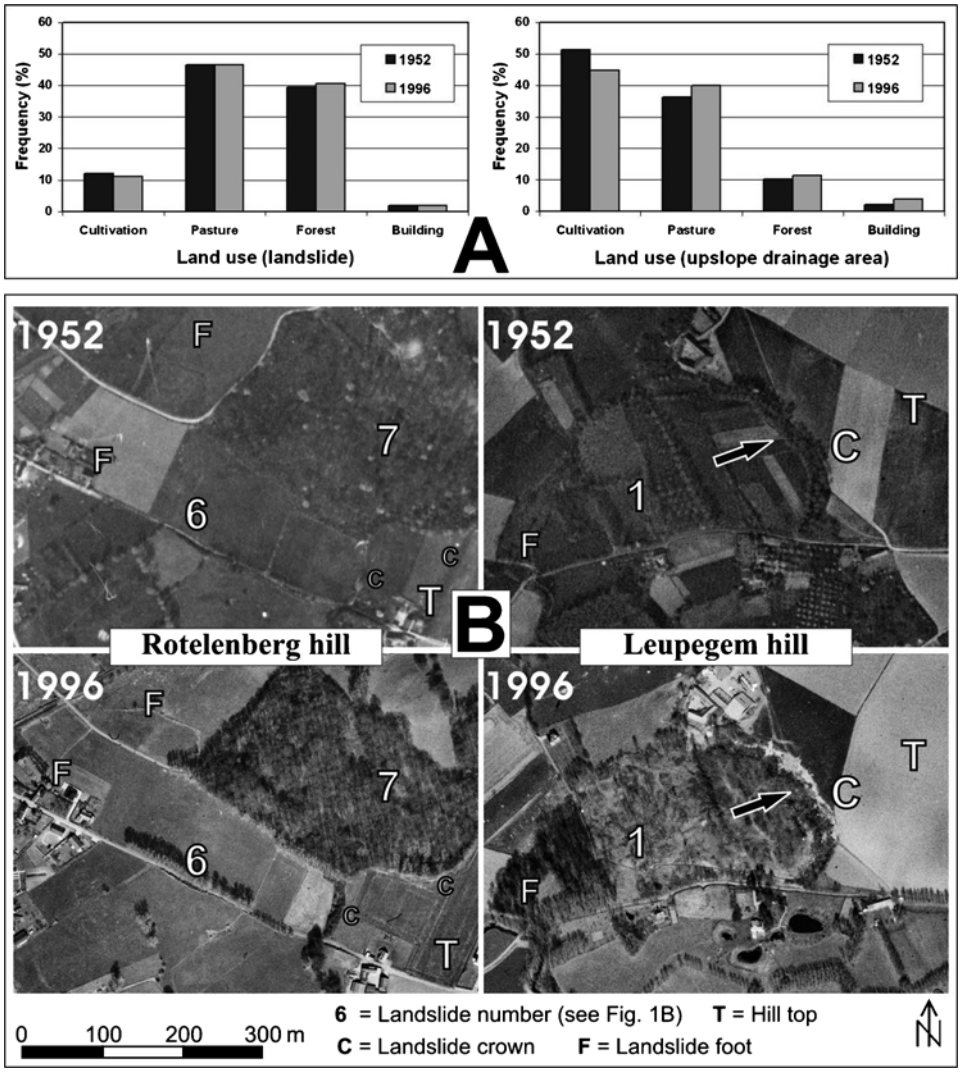

Fig. 2. (A) Land use changes between 1952 and 1996. Land use is shown for all the area covered by the landslides (left view) and the area upslope of the main scarps draining the landslides (right view). (B) Land cover changes of a part of the Rotelenberg hill (landslide 6 and 7) and the Leupegem hill (landslide 1) between 1952 and 1996. The black arrows indicate the main scarp of landslide 1.

3 *Material and methods: DTM subtraction*

Reconstructing landslide topography at different dates allows, by simple DTM subtraction, differences in elevation at each landslide pixel to be identified, which may depend on vertical and horizontal landslide movements during the considered time interval (Oka 1998, Weber and Herrmann 2000, Gentili et al. 2002, Kääb 2002, van Westen & Getahum 2003, Baldi et al. 2005, Hapke 2005, Lantuit & Pollard 2005, Brückl et al. 2006, Demoulin 2006).

The DTM used for the ground movement detection was computed by Dewitte et al. (2008). The topographic data used for the DTM interpolation were collected by aerial digital stereophotogrammetry. The aerial photographs (1952, 1973 and 1996), at scales between 1:18,500 and 1:25,000, were all taken at the beginning of the spring (when the trees are leafless), and the photograph negatives were scanned with a precision scanner at a pixel resolution of 12.5 μm that corresponds to a ground resolution of ~ 20–30 cm (Dewitte et al. 2008). The image processing was performed with LH Systems SOCET SET software. The interior orientation was performed by using the parameters of the camera established by the geometric calibration. Three precise aerotriangulations of the obtained digital photos (1996, 1973, 1952) were then carried out by using the bundle block adjustment method that allows simultaneously the relative and the absolute orientations of the photographs in the block (Mikhail et al. 2001). The block adjustment accuracy was evaluated using check points acquired by differential GPS in rapid static mode involving baselines of a few km length, but not used as control in the solution. The final uncertainty on the coordinates of the check points does not exceed 10 cm. The first stereomodel was adjusted with the photographs of 1996 and ground control points also acquired by differential GPS with the same uncertainty as that of the check points. To avoid inaccuracies associated with the positioning of these ground control points, the two stereomodels of 1973 and 1952 were rectified relative to the 1996 stereomodel by including the orientation parameters of 1996. The global root mean square error (RMSE) obtained for the three stereomodels range between 22 cm and 55 cm.

The stereoscopic data capture of spot heights (ground points) and breaklines (scarps, roads, water bodies) on the landscape surface was carried out visually since the automatic terrain extraction methods provided with SOCET SET were not able to generate DTMs sufficiently accurate in many places, especially in the forested areas (Dewitte et al. 2008). The spot heights were extracted approximately every 10 m, but with a higher density in more contrasted topography, in particular within the landslides.

The captured elevation data were interpolated by ordinary kriging with adjusted semivariograms (Dewitte et al. 2008). Taking into account the data density, their spatial autocorrelation shown by the semivariograms, and the precision and the accuracy of the stereomodels, six DTMs (3 different dates for each investigated hill (fig. 1B)) were generated at a 2 m resolution with a final RMSE of ~ 0.55 m (table 1). When DTMs are subtracted, their errors can be combined as independent random variables, and under the assumption of normal distribution, the combined error can be used as standard deviation (Mikhail et al. 2001). Therefore DTM subtraction allows to capture differences in elevation of ~ 0.70 m or larger at a 68.3 % confidence level (table 1).

Table 1. DTM accuracies and confidence intervals of the DTM subtraction. These mean values are synthesized from Dewitte et al. (2008).

Year	1996	1973 (m)	1952
DTM Accuracy			
Z RMSE*	0.45	0.45	0.52
XY RMSE**	0.17	0.28	0.42
XYZ RMSE	0.48	0.53	0.67
DTM Subtraction			

Confidence intervals	68.3 %		95 %	
	XY (m)	Z (m)	XY (m)	Z (m)
	± 0.67	± 0.67	± 1.06	± 1.31

Several morphological features such as unvegetated scarps and tilted trees (Van Den Eeckhaut et al. accepted) witness to recent movements in almost all the landslides. With visible displacements of at least 6–7 m, the reactivation of landslide 1 in February 1995 (Van Den Eeckhaut et al. 2007 a), easily identified on aerial photographs (fig. 2B), is the most important movement recorded recently within the study area (Dewitte 2006). However, in general, the movements observed in the field appear rather small (in the order of a few meters) and slow. The use of DTMs therefore allows for the quantification of most of them. Moreover, with a 44-year period of observation, the differential DTMs can capture relatively larger-sized movements and allow for the evaluation of the cumulative effects of single or multiple landslide events.

4 *Results: landslide ground movements*

4.1 *Vertical movements*

The vertical ground displacements measured between 1952 and 1973, 1973 and 1996, and 1952 and 1996 are presented in figs. 3, 4 and 5 respectively. These differential maps are produced with a confidence value of ± 0.70 m that corresponds to the confidence interval of 68.3 % resulting from the DTM subtraction (table 1), which means that only differences in elevation higher than 1 σ uncertainty are shown. Therefore, small vertical displacements between two successive epochs may add to appear only on the 1952–1996 map if their sum > 0.70 m. Conversely, significant displacements of opposite sign in the two successive periods may cancel out in the 1952–1996 map.

Ground movements are observed in all landslides and, for the most active of them (i. e. landslides 1, 2, 4, 6 and 7), the movement pattern is typical of rotational deep-seated failures (figs. 3, 4 and 5) with subsidence in the zone of depletion and uplift within the zone of accumulation. Such a pattern might be due, in part, to the

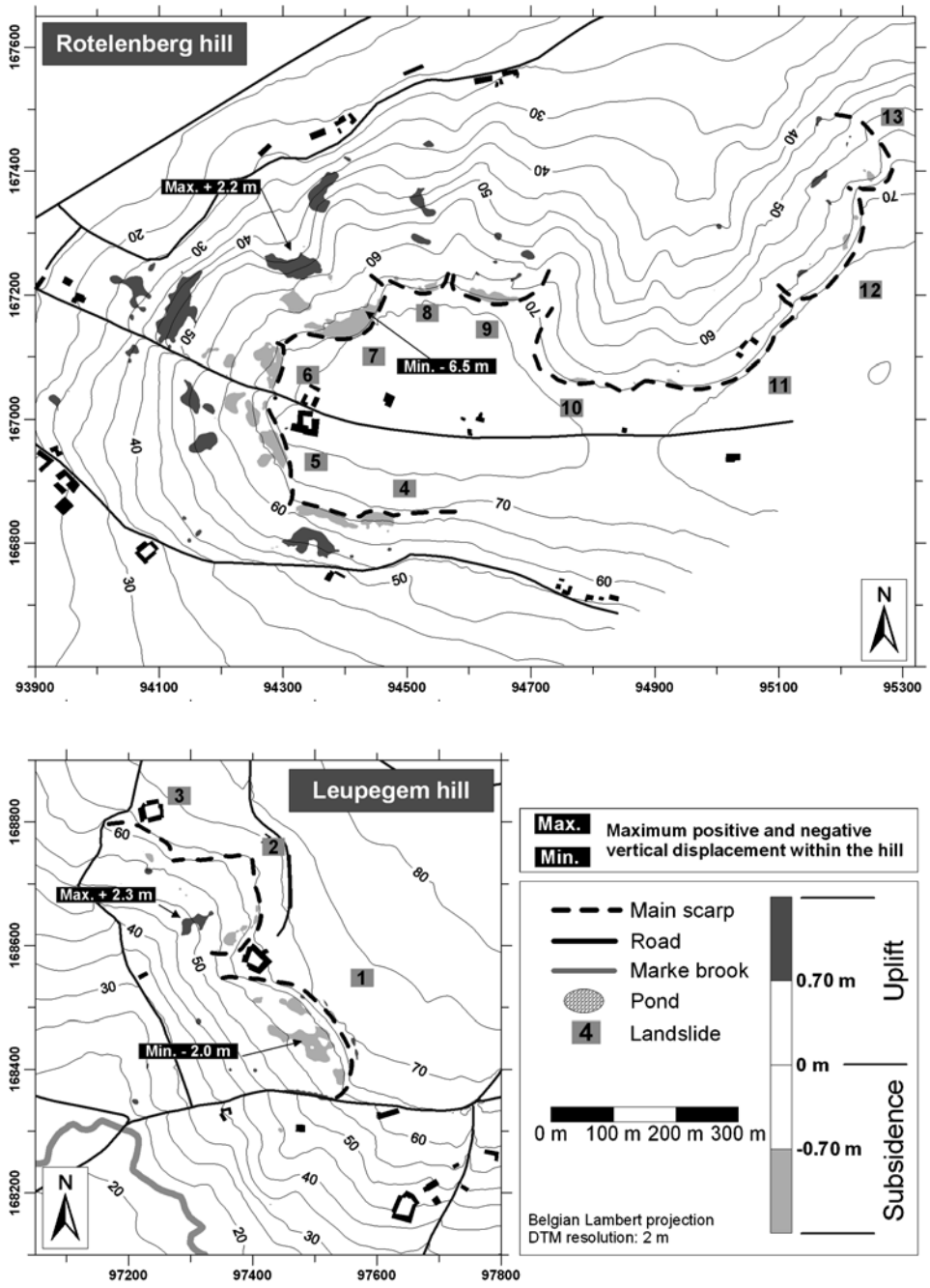

Fig. 3. Vertical ground displacements within the Rotelenberg and the Leupegem hills inferred from subtraction of detailed DTMs produced from aerial photographs of 1973 and 1952. Only the vertical movements in excess of ± 1 σ (i. e. ± 0.70 m) uncertainty are represented. The underlying contour lines describe the topography of 1973.

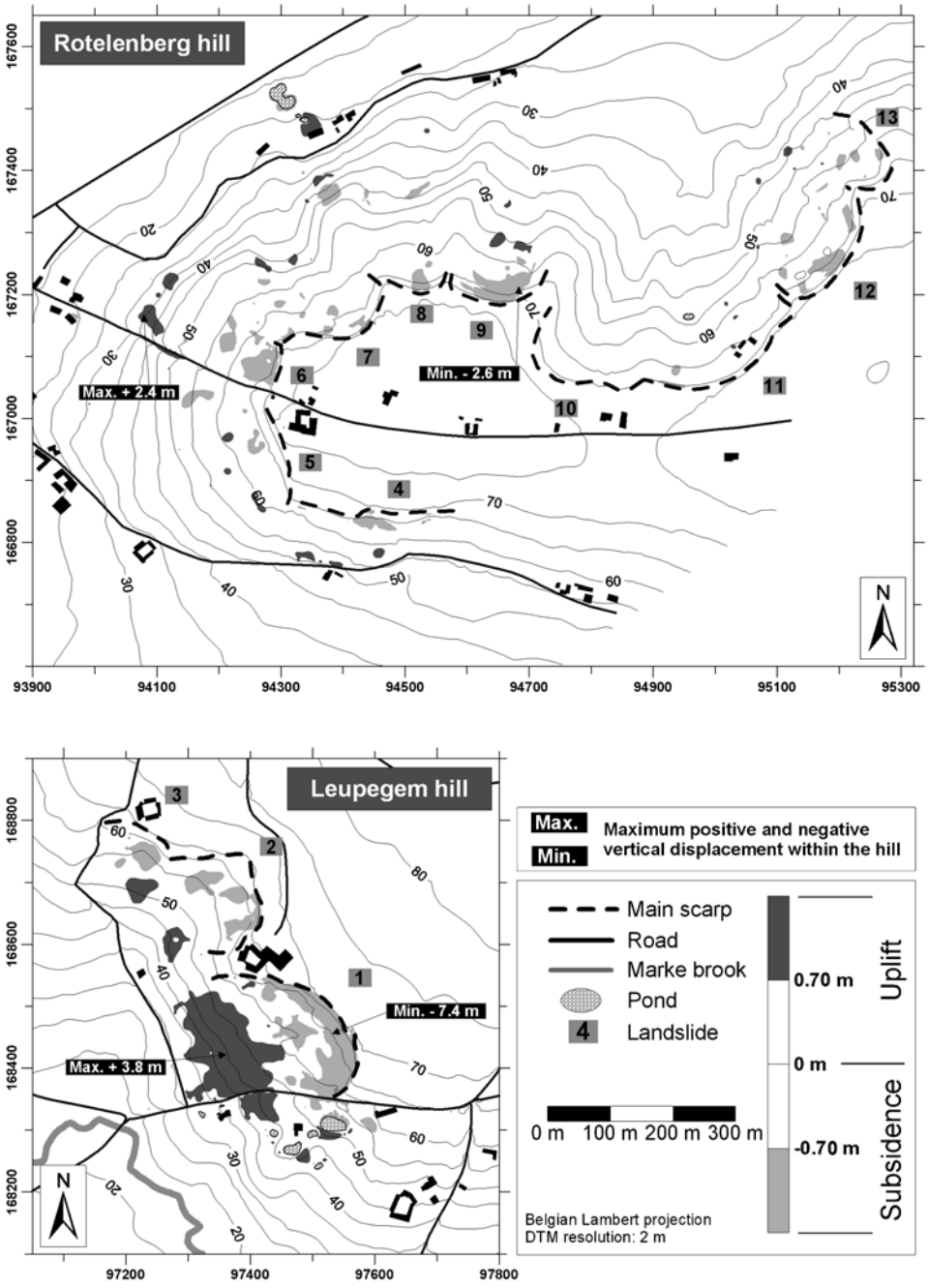

Fig. 4. Vertical ground displacements within the Rotelenberg and the Leupegem hills inferred from subtraction of detailed DTMs produced from aerial photographs of 1996 and 1973. Only the vertical movements in excess of ± 1 σ (i. e. ± 0.70 m) uncertainty are represented. The underlying contour lines describe the topography of 1996.

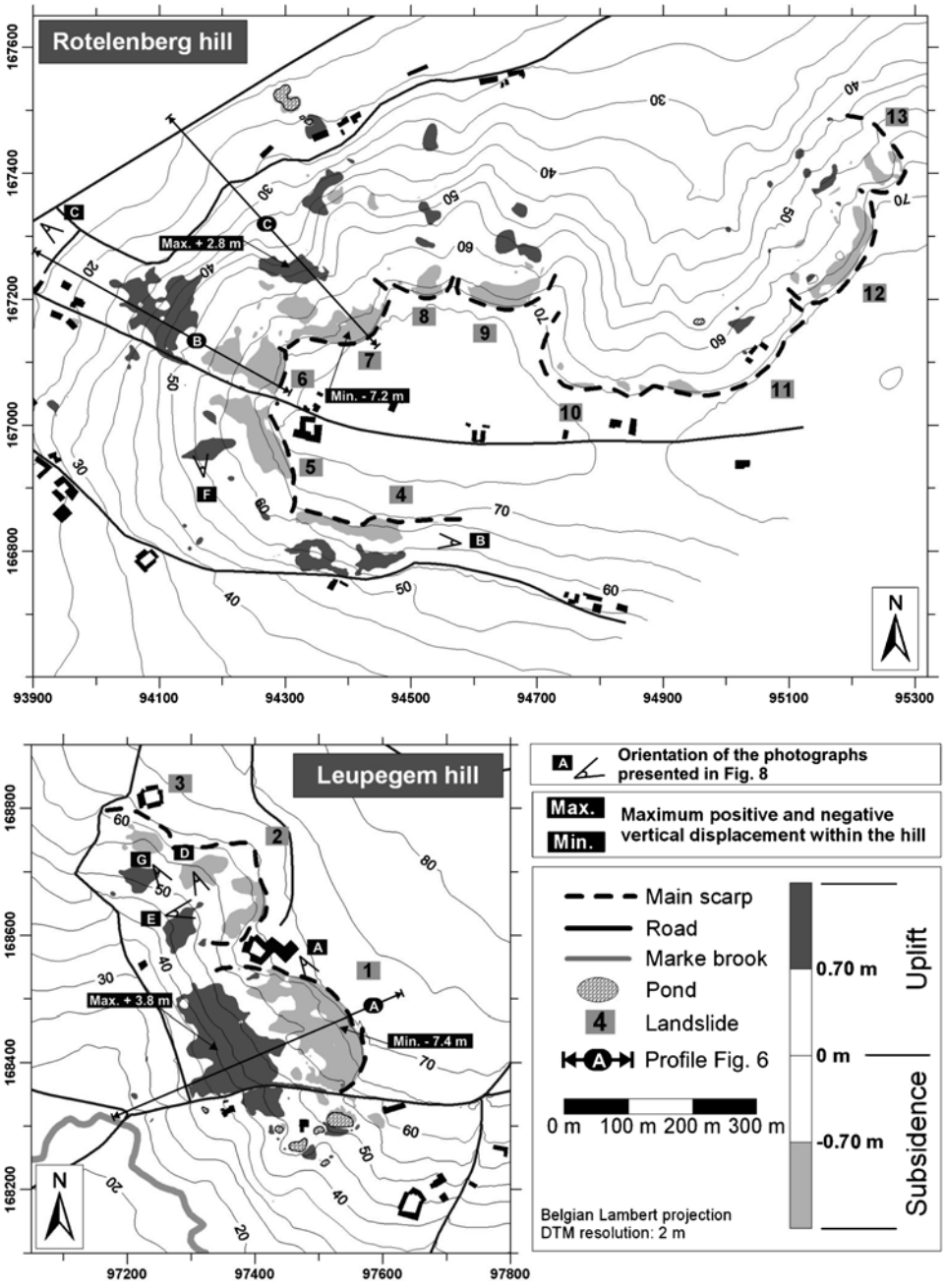

Fig. 5. Vertical ground displacements within the Rotelenberg and the Leupegem hills inferred from subtraction of detailed DTMs produced from aerial photographs of 1996 and 1952. Only the vertical movements in excess of ± 1 σ (i. e. ± 0.70 m) uncertainty are represented. The underlying contour lines describe the topography of 1996. Lettered black lines A, B, and C locate the profiles of fig. 6.

reactivation of pre-existing slides. Whereas landslides 10 and 11 are almost stable, vertical ground motions, both positive and negative, are detected in the landslides with the largest movements. In the less active landslides (3, 5, 8, 12 and 13), the movements consist mainly of subsidence at the head. While some landslides (e. g., 4 and 6) were active during the two periods, others moved mainly between either 1952 and 1973 (e. g., 7) or 1973 and 1996 (e. g., 1).

In landslide 6, the downslope uplift was more important than the subsidence at the head before 1973 (fig. 3), a situation opposite to that after 1973 (fig. 4). Since subsidence should precede uplift, this particular evolution could be partly related to a delayed response to the pre-1952 activity of the landslide (van Westen & Getahun 2003). It may suggest that this landslide is complex or compound, and not simply a rotational slide, the 1952–1973 uplift (fig. 3) following a pre-1952 subsidence, and the 1973–1996 subsidence being not entirely compensated by the downslope uplift (fig. 4). The two adjacent areas of subsidence between 1952 and 1996 in the zone of depletion suggest multiple rotational movements within this currently active landslide (fig. 5).

With movements of up to 7.4 m in the zone of depletion and 3.8 m in the zone of accumulation, landslide 1, which was deeply reactivated in February 1995 after a period of intense rainfall (Van Den Eeckhaut et al. 2007 a), is by far the most active feature of the study area (figs. 4 and 5). The large vertical motion at its head corresponds fairly well to the height of the retreating scarp. The displacements within landslides 1 occurred almost exclusively during the 1973–1996 interval; the largest movement being the February 1995 reactivation (Dewitte et al. 2008, Van Den Eeckhaut et al. 2007a).

The vertical motions observed in landslide 7 are very similar to those detected in landslide 1, but they developed mainly between 1952 and 1973, with maximum displacements ranging between – 6.5 m and + 2.2 m (fig. 3).

Several other displacements seem to have developed independently of the presence of the old landslides and, therefore, are not considered as reactivation (e. g., the rotational failure located around 40 m a. s. l. between the zones of accumulation of landslides 7 and 8, and the uplift in landslide 11 around 60 m a. s. l. (fig. 5)).

4.2 *Horizontal movements*

As stressed by Dewitte et al. (2008) in the study of landslide 1, topographic profiles are very illustrative of the combination of vertical and horizontal displacements (fig. 6A). In this landslide, the distribution of the topographic variations recorded between 1952 and 1996 corresponds to a rotational angle dividing the landslide in three areas, respectively of depletion, transfer and accumulation, in agreement with the conceptual model developed by Casson et al. (2005) for rotational landslides. According to this model and considering the distribution of elevation changes, the morphometric characteristics of the landslide obtained by Dewitte & Demoulin (2005), and the lithological context (i. e. the alternation of the subhorizontal clayey sand and clay layers), Dewitte et al. (2008) located the surface of rupture of the February 1995 reactivation at a depth of ~ 20 m partly in contact with the Aalbeke clays. The surface of rupture stretches over a horizontal length of 220 m. This shows that the uplift in the zone of accumulation is not a true vertical movement of the ground,

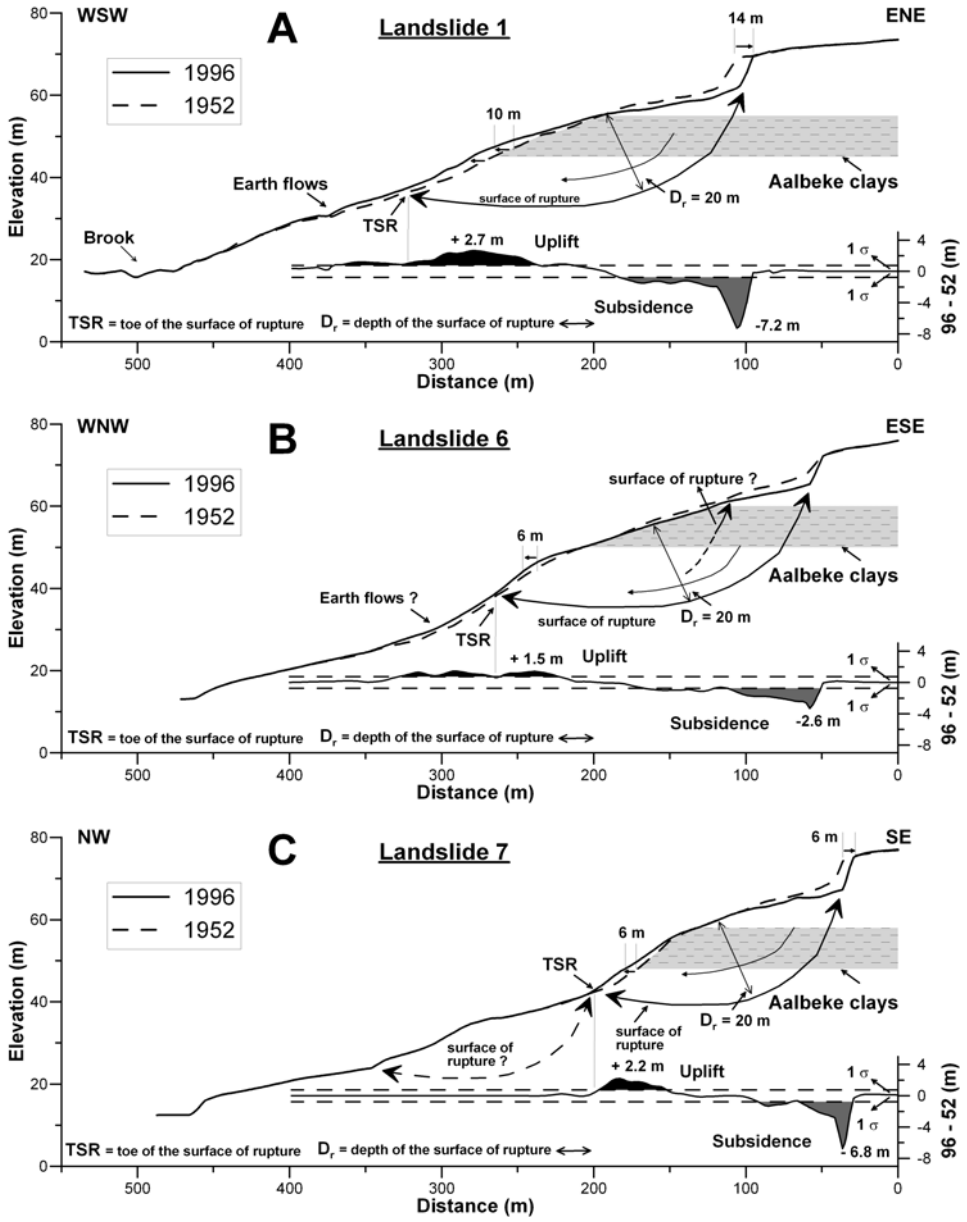

Fig. 6. Topographical profiles across the landslides 1, 6, and 7 illustrating the 1952–1996 vertical motions. The lateral motion of the main scarps and ridges are also represented (horizontal arrows). The curve associated with the second Y-axis (on the right) corresponds to the vertical movements extracted from the subtraction of the 1952 topography to that of 1996. The empty area between the two horizontal dashed lines delimits the ± 1 σ confidence band resulting from the DTM subtraction. Only the vertical movements in excess of ± 1 σ (i. e. 0.70 m) uncertainty are represented, locating the collapsed and uplifted parts. For each curve, the maximum and minimum vertical movements are noted. The three profiles are located on fig. 5.

but mainly the effect of the downslope lateral displacement of the mass slipping along the curved rupture surface (fig. 6A). Due to the movement along this curved surface of rupture, the horizontal component of this displacement is therefore lower than the horizontal distance between the two profiles (10 m) that would result from a movement on a horizontal sliding plane. In the same way, the transfer area where no vertical displacement of the surface is observed between the areas of subsidence and uplift corresponds to a zone of mainly horizontal but smaller motion.

Based on field observations reported by Van Den Eeckhaut et al. (2007a), Dewitte et al. (2008) demonstrated that small uplifts downslope of the toe of the surface of rupture (i. e. at the intersection between the lower part of the surface of rupture and the original ground surface) were induced by small earth flows following the main reactivation (fig. 6A). The similar patterns of the elevation changes in landslide 1 and landslides 6 and 7 (fig. 5) suggest that the latter failures were of the same nature as the 1995 event in landslide 1. In addition, the topographic profiles of figs. 6B and C show that the model of rotational movement proposed by Casson et al. (2005) can be applied to landslides 6 and 7 as well. As for landslide 1, their surface of rupture is in contact with the Aalbeke clays at a depth of ~ 20 m, with horizontal lengths of respectively ~ 200 m and ~ 170 m. Uplift in the zone of accumulation of landslides 6 and 7 does not represent a true vertical ground movement, but is rather an effect of the downslope displacement (figs. 6B and C).

Electric resistivity profiles measurements carried out across a similar but dormant rotational earth slide by Van Den Eeckhaut et al. (2007c) revealed a surface of rupture at a depth of 15 m, comparable to that found for the reactivations. Moreover, the surface of rupture was also in contact with the sensitive clays of the Aalbeke Member. This confirms that the deep reactivations affected pre-existing shear surfaces. The position of the surface of rupture along the Aalbeke clays (fig. 6) may be subject to imprecision due to the thickness of the clay Member which may range between 3 m and 15 m over distances of a few hundred meters only (Jacobs et al. 1999). In addition, a few meters uncertainty is also associated with the estimation of the depth of the surface of rupture. The shape of the surface of rupture as well as the presence of horizontal sediment layers do not exclude that part of the motion in the toe of the surface of rupture primarily occurred as translational sliding, as evidenced for similar landslides in eastern Belgium (Demoulin et al. 2003).

Furthermore, in landslide 6, a second surface of rupture can be drawn between two distinct areas of subsidence, thus dividing the zone of depletion into two blocks, and earth flows are present downslope of the toe of the surface of rupture (fig. 6B). The morphology of the zone of accumulation within landslide 7 differs from those of landslides 1 and 6, possibly as a result of a reactivation of the whole foot (fig. 6C). This movement occurred before the 1952–1973 reactivation, but it is not clear whether during the landslide initiation event or in a later phase of reactivation.

The topographic profiles clearly illustrate that the location of the main scarps at the edge of the horizontal hill top and show that the zones of highest subsidence in the zone of depletion are related to the retreat of the main scarp and can correspond to its height (e. g., landslides 1 and 7). Therefore, the width of the subsidence area may be interpolated in terms of a horizontal motion of scarp retreat. For landslides 1 and 6, it amounts to respectively 14 m and 6 m along the slope profile (fig. 6). These values are fairly accurate since they are extracted from visually well-identifiable geomor-

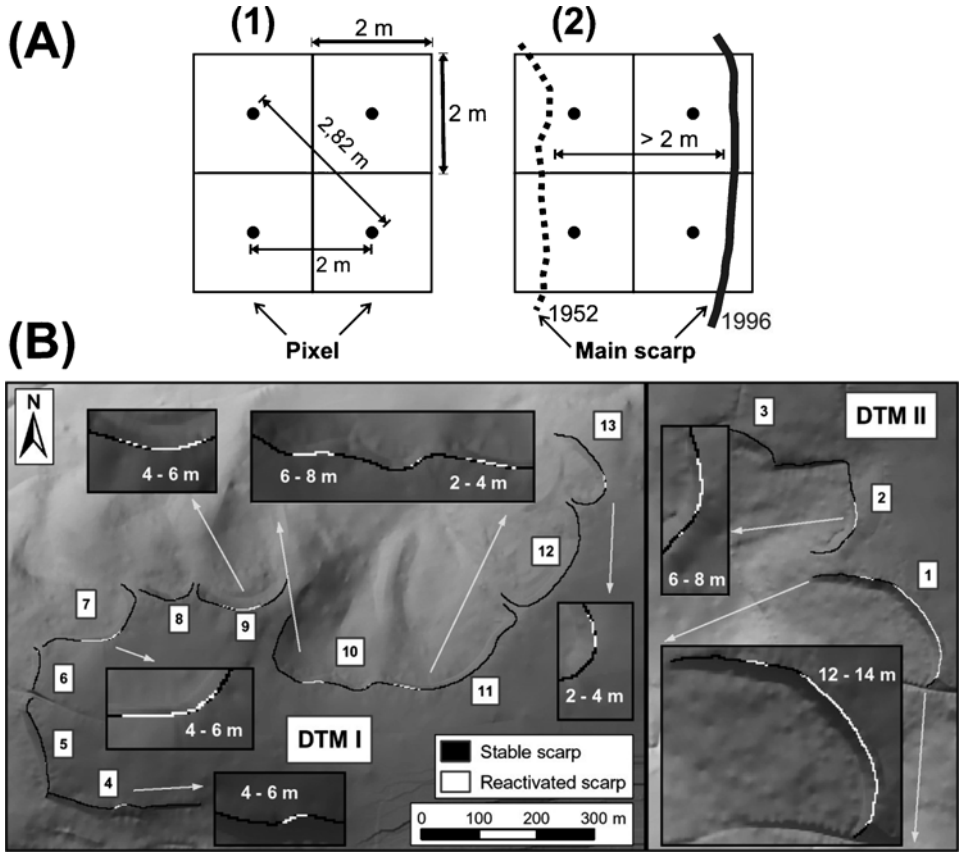

Fig. 7. (A) Measurement of the horizontal displacements at the main scarps. (1) Euclidian distance between two pixel centres (black dots). (2) Horizontal distance between a main scarp in 1952 and its position in 1996. (B) Retreat of the main scarps between 1952 and 1996 (horizontal scarp retreat > 2 m). The values represent the maximum retreat in meters measured at each scarp. The retreats are located with a confidence interval > 95 %.

phologic features (Gentili et al. 2002). Spatial and temporal heterogeneities of head scarp retreat are also observed (Dewitte 2006). Due to these heterogeneities and in order to limit the discussion to the most reliable movements, we only considered the total scarp retreat from 1952 to 1996 (fig. 7A).

We computed it after rasterization of the main scarps at a 2 m resolution, similar to that of the DTMs. Therefore, a scarp was said reactivated if its retreat was > 2 m. The retreat amount was computed as the 2D Euclidian distance between pixel centres (fig. 7A1). This threshold value fits very well with the XY accuracy of the DTMs (table 1), so that the mapped scarp retreats are all significant at the 95 % confidence level. Nevertheless, the smoothing of the main scarps due to the rasterization might give rise to marginally biased retreat values. For example, a retreat > 2 m in reality (fig. 7A2) might, after rasterization, be converted into a displacement of 2 m

and therefore not considered as significant. The observed scarp retreats range from 0 to 14 m over the 1952–1996 period (fig. 7B), with the highest value in landslide 1. The largest motions in the Rotelenberg hill amount to 8 m (fig. 7B). The scarp retreat of landslide 1 is clearly related to its reactivation in February 1995. Photograph and field interpretation also attest the landslide 4 scarp retreat as a consequence of its pre-1996 reactivation, and the DTM measurements show that the scarp retreat of landslide 7

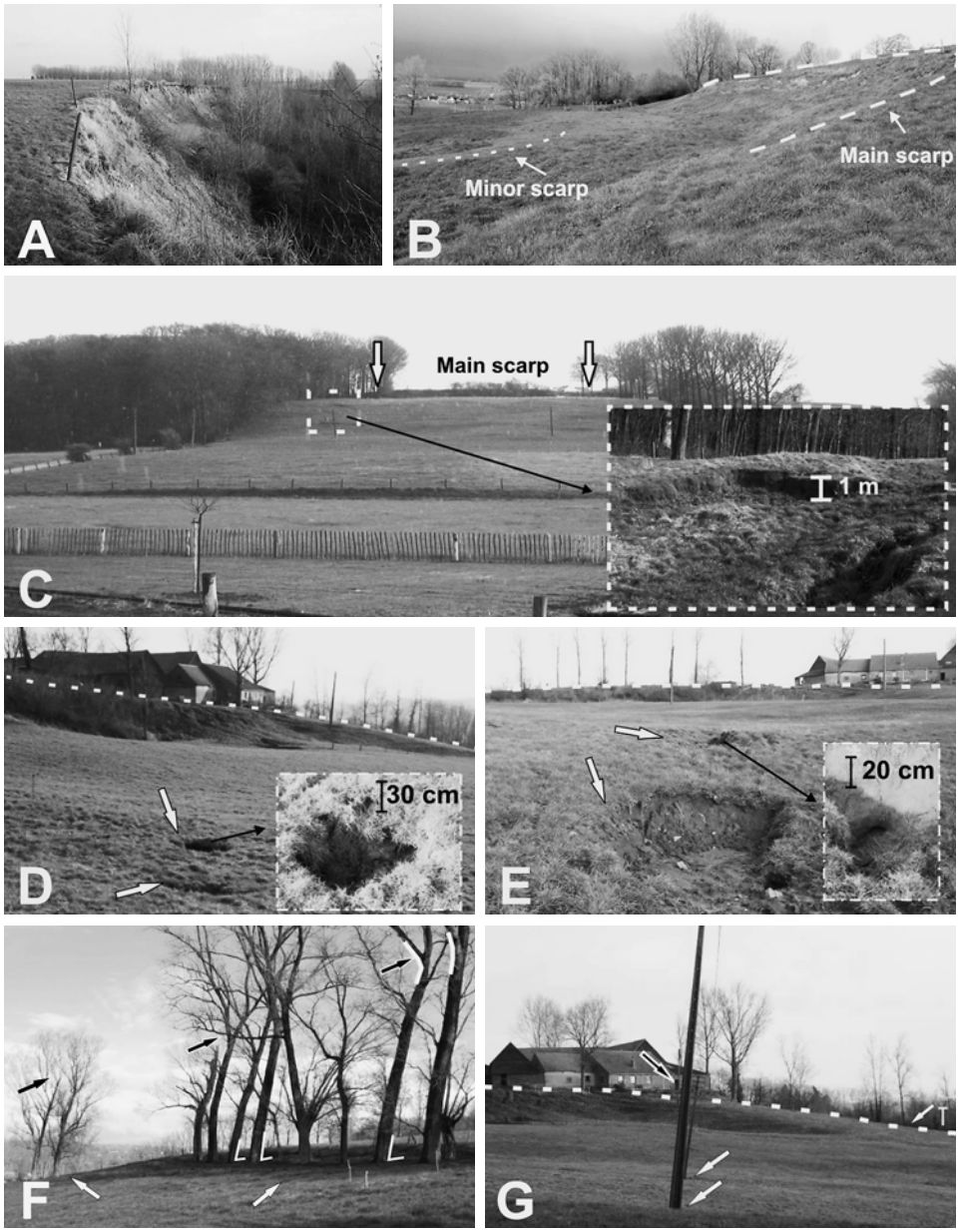

occurred mainly during the 1952–1973 interval. However, it is less clear whether the other retreats have to be associated with reactivation or slope instability independent of the large landslides.

4.3 *Field validation*

The presence of sharp main scarps, undrained depressions at landslide heads, hummocky topography, and trees tilted or bent suggests a historic (< 100 years) or late Holocene activity of the landslides (Keaton & DeGraff 1996) and support to movements detected by DTM subtraction (fig. 8), as also do traces of damage to infrastructures (road, house) in landslide 1. The sharp and partly unvegetated main and minor scarps of landslide 4 (fig. 8B) bear witness to movements developed just before 1996 (fig. 4); these features being not visible on the pre-1996 photographs. Likewise, minor unvegetated scarps (fig. 8C) in landslide 6 indicate pre-1996 reactivation. Piping and tilted electricity poles demonstrate the recent activity of landslide 2 (figs. 8D, E, and G), as tilted and bent trees in landslide 5 too (fig. 8F). Partly unvegetated transverse ridges witnessing shallow failure extend in the uplift area at ~ 60 m a. s. l in landslide 11. Moreover, some features have been obliterated by agricultural activities. For example, a part of the displaced material within the zone of accumulation of landslide 5 was levelled (Dewitte 2006) and therefore not detected on the DTMs (fig. 4). Similarly, in forest, tilted trees are frequently cleared.

5 *Discussion*

Based on the DTM measurements and the field observations, the movements within the landslides can be split into two groups. The first group comprises the reactivations of the landslides, linked to their retrogressive behaviour. Some of them affect the landslides at depth (landslides 1 and 4, and possibly also 6 and 7) (fig. 6). These reactivations partly re-use pre-existing surface of rupture and affect both the main scarp and the zone of accumulation. Similar reactivations may have occurred within landslides that look less active (i. e. landslides 3, 5, 8, 12 and 13). The analysis with a

Fig. 8. Traces of recent movements within the landslides. The position of the photographs is indicated in fig. 5. (A) View towards the SE of the February 1995 reactivated main scarp of landslide 1 (February 2003). (B) View towards the W of the reactivated main scarp of landslide 4 (April 2004). The lateral extension of the main scarp is ~ 60 m. (C) View towards the SE from the tip of landslide 6 in which a unvegetated minor scarp (dashed rectangle) is located (April 2004). The main scarp is ~ 80 m length. (D) and (E) Examples of piping observed in landslide 2 (view towards the SE (A) and the E (B), February 2003). The white arrows indicate pipe entrances or collapses and the dashed line shows the main scarp. (F) Example of tilted trees (view towards the N, landslide 5, April 2004). The white arrows show tilted trees toppled backward towards the landslide main scarp. The black arrows indicate bends at the top of these trees. The white dashed line marks a minor scarp. (G) Example of tilted electricity poles (view towards the SE, landslide 2, February 2003). The two white arrows at the front indicate tilted poles, and the black and white arrow at the back shows a stable one. The white arrow with letter "T" at the back of the view indicates a tree in landslide 1 tilted upslope. The white dashed lines indicate scarps: the main scarp is at the back of the view and two minor scarps at the front.

LIDAR DTM of the ground movements of landslide 1 after it reactivated (i. e. after 1996) stressed, in agreement with field observations, the importance of the compaction of the displaced material within the zone of accumulation and showed how this process can reduce significantly the uplift associated with a reactivation (Dewitte et al. 2008). This could explain why within these landslides the movements consist mainly of subsidence in the zone of depletion, suggesting that they might have been reactivated at a time that allowed compaction to act.

The second group of movements consists of all displacements that do not correspond to reactivation, including the earth flows in the zone of accumulation of landslides 1 and 6 (fig. 6) and other small features. Similar earth flows could perhaps have caused displacements in the zone of accumulation of landslides 5, 8 and 9 (figs. 4 and 5).

Obviously rainfall triggered most of the displacements detected between 1952 and 1996. Numerous studies have shown the importance of a period of several weeks or months with intense rainfall for triggering reactivations of old landslides developed in clayey sediments (Polemio & Sdao 1999, Fiorillo 2003, Demoulin & Glade 2004, Cubito et al. 2005, Demoulin 2006), which clearly correspond to what was observed for landslide 1 reactivation (Van Den Eeckhaut et al. 2007 a). The landslide started to move in early February after two wet months in December 1994 and January 1995. Compared with the long-term averages of 69, 62, and 51 mm, rainfall depths of respectively 126.7, 168.2, and 115.3 mm were recorded at Oudenaarde this year, and, considering a period of ~ 50 days before the reactivation, the cumulative rainfall depth rises to ~ 265 mm, which corresponds to a recurrence of ~ 40 years (Dupriez & Demarée 1989), i. e. well above the monthly threshold of 100 mm computed by Van Den Eeckhaut (2006) for landslide reactivation in the Flemish Ardennes.

Despite such an intense rainfall period, only landslide 1 was reactivated and no significant displacement was observed at that time elsewhere in the study area. The reconstruction of the landslide 1 activity by Van Den Eeckhaut et al. (2007 a) suggests that anthropogenic preparatory factors played an important role in its reactivation. The upper part of the landslide was cultivated until 1955 thanks to a drainage system. In 1955, the agricultural activities were stopped and the drainage channels were no longer maintained, resulting probably in an increased shear stress (due to the weight of groundwater) and decreased shear strength (due to the higher pore pressures). Shear stress was further increased by additional loading due to the artificial elevation of the road in order to improve the accessibility (see the vertical uplift along the road crossing landslide 1 (fig. 3)); this road also hampers drainage. Local loading associated with garden construction has also to be mentioned (fig. 4). Moreover, in the area upslope of landslide 1, the parcel size increased significantly (figs. 2B and 9A) and the growing of maize since the eighties has caused an increase in surface runoff towards the landslide, as witnessed by the initiation of gully erosion at the scarp (fig. 9B).

The other large reactivations such as those of landslides 4 and 6 do not seem to have been so closely associated with anthropogenic factors. Unfortunately no precise date of movement is available to derive the associated amount of rainfall.

Rainfall also triggered other movements (Dewitte et al. 2008, Van Den Eeckhaut et al. 2007a). For example, the small subsidences observed at the head of landslide 1 between 1952 and 1973 (fig. 3) might have resulted from destabilization and

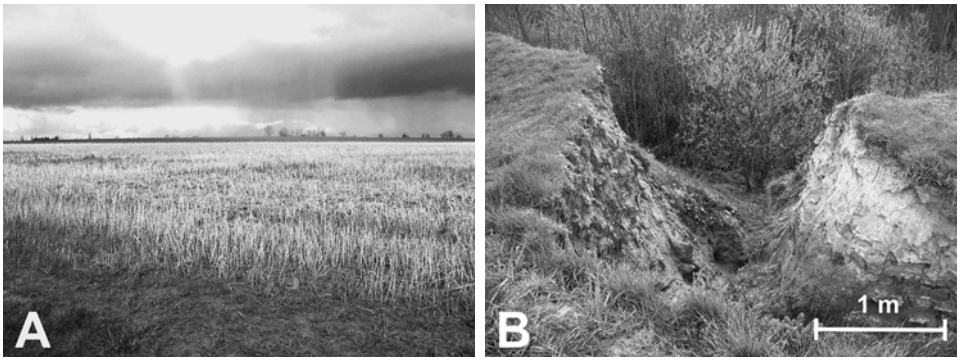

Fig. 9. (A) Large cultivated area upstream of the main scarp of landslide1. Mainly in winter, the bare soils favour surface runoff and then flow concentration towards the landslide (Leupegem hill, April 2004; view towards the N). (B) Gully erosion in the main scarp of landslide 1. This gully results from the concentration of the surface runoff developed in the large cultivated plot (Leupegem hill, April 2004; view towards the SW).

tension cracks in response to high groundwater levels at the contact with the Aalbeke clays and small movements in this area were observed in 1960 and 1966 after several wet months.

Vegetation is a further control on the occurrence of some movements. For example, in 1955, the trees along the main scarp of landslide 1 were cut down and replaced by young poplar trees (Van Den Eeckhaut et al. 2007a). Assuming a first period of root decay followed by the slower recovery of root strength after replanting (Schmidt et al. 2001, Sidle et al. 2006), this could explain why, 5 years after tree removal, small movements were observed in 1960 close to the main scarp (fig. 3). More generally, with regard to the landslide activity, it seems that the forested areas (mainly beech and poplar trees) favour hillslope stabilization due to increasing shear strength (landslides 8, 9, 11, 12 and 13) (Sidle et al. 2006), although this should be less efficient against reactivation at depth (Van Den Eeckhaut et al., accepted). In addition, higher evapotranspiration of the forest may act to stabilize hillslopes by drying soils (Verstraeten et al. 2005, Sidle et al. 2006). Deep-rooted vegetation species growing in deep soils sustain high transpiration rates for long periods, thus drying soils at greater depths compared to shallow-rooted vegetation, and decreasing landslide potential (Sidle et al. 2006). The higher activity of some forested landslides (landslide 7) may be due to anthropogenic disturbances such as timber harvesting (Montgomery et al. 2000, Schmidt et al. 2001) as suggested by the destructured appearance of the 1952 forest of the Rotelenberg hill (fig. 2B).

Piping is observed within the main body of landslide 2 (figs. 8D and E). It could have contributed to some local collapses (figs. 3 and 5) although the role of piping on slope stability remains unclear (Uchida et al. 2001). No other pipe was observed in the study area (Dewitte 2006).

6 *Conclusions*

This study aimed at providing a better understanding of the mechanisms and the controlling factors of the ground movements occurring within the old landslides of the Flemish Ardennes. With the use of reliable multi-temporal 2 m-resolution DTMs, the study of 13 old landslides representative of the Flemish Ardennes has demonstrated that ground movements occurred in all of them during a period of 44 years. The setting and the magnitude of the displacements vary spatially and temporally. Within the most active landslides, the movement pattern is typically rotational deep-seated failure with subsidence in the zone of depletion and uplift within the zone of accumulation. However, a detailed analysis of the vertical and horizontal movements allowed us to recognize various slope processes and the related controlling factors.

We distinguished between reactivation and non-reactivation features. Some reactivations are large and affect the landslides in depth by re-using pre-existing surface of rupture. These reactivations are associated with the largest amounts of subsidence and uplift. Smaller reactivations are more confined and only affect the landslide head. These findings suggest a retrogressive activity of multiple rotational earth slides.

The other measured displacements consist in (1) earth flows occurring in the zone of accumulation, sometimes as a consequence of a large reactivation and (2) small failures occurring independently of the presence of the old landslides.

Most movements were triggered by intense rainfall, and differences in their controlling factors explain their spatial and temporal distribution: (1) vegetation clearly reduces the potential for shallow failures in the forested parts due to increase in shear strength, and (2) anthropogenic activities change the probability of movement occurrence.

Our results support the hypothesis that slope movements affect more frequently the old landslides of the Flemish Ardennes than the archive analysis let suggest. They stress the need for considering old landslides in land management and mitigation strategies in hilly areas, even if they look stabilized.

References

Agnesi, V., Camarda, M., Conoscenti, C., Di Maggio, C., Diliberto, I.S., Madonia, P. & Rotigliano, E. (2005): A multidisciplinary approach to the evaluation of the mechanism that triggered the Cerda landslide (Sicily, Italy). – Geomorphology **65**(1–2): 101–116.

Baldi, P., Fabris, M., Marsella, M. & Monticelli, R. (2005): Monitoring the morphological evolution of the Sciara del Fuoco during the 2002–2003 Stromboli eruption using multi-temporal photogrammetry. – ISPRS J. of Photogrammetry and Remote Sensing **59**(4): 199–211.

Bentley, S.P. & Siddle, H.J. (1996): Landslide research in the South Wales coalfield. – Engineering Geology **43**(1): 65–80.

Brückl, E., Brunner, F.K. & Kraus, K. (2006): Kinematics of a deep-seated landslide derived from photogrammetric, GPS and geophysical data. – Engin. Geol. **88**(3–4): 149–159.

Casson, B., Delacourt, C. & Allemand, P. (2005): Contribution of multi-temporal remote sensing images to characterize landslide slip surface – Application to the La Clapiere landslide France). – Natural Hazards and Earth System Sciences **5**(3): 425–437.

Cubito, A., Ferrara, V. & Pappalardo, G. (2005): Landslide hazard in the Nebrodi Mountains (Northeastern Sicily). – Geomorphology **66**(1–4): 359–372.

De Moor, G. & Pissart, A. (1992): Les formes du relief. – In: Denis, J. (Ed.), Géographie de la Belgique. Crédit communal de Belgique, Bruxelles, pp. 129–216.

Demoulin, A. (2006): Monitoring and mapping landslide displacements: a combined DGPS-stereophotogrammetric approach for detailed short- and long-term rate estimates. – Terra Nova **18**(4): 290–298.

Demoulin, A. & Glade, T. (2004): Recent landslide activity in Manaihan, East Belgium. – Landslides **1**(4): 305–310.

Demoulin, A., Pissart, A. & Schroeder, C. (2003):. On the origin of late Quaternary palaeolandslides in the Liege (E Belgium) area. – Internat. J. of Earth Sciences **92**(5): 795–805.

Dewitte, O. (2006): Kinematics of landslides in the Oudenaarde area and prediction of their reactivation: a probabilistic approach. – Ph. D. Thesis, University of Liège, Liège, 213 pp.

Dewitte, O., Chung, C.-J. & Demoulin, A. (2006): Reactivation hazard mapping for ancient landslides in West Belgium. – Natural Hazards and Earth System Sciences **6**(4): 653–662.

Dewitte, O. & Demoulin, A. (2005): Morphometry and kinematics of landslides inferred from precise DTMs in West Belgium. – Natural Hazards and Earth System Sciences **5**(2): 259–265.

Dewitte, O., Jasselette, J. C., Cornet, Y., Van Den Eeckhaut, M., Collignon, A., Poesen, J. & Demoulin, A. 2008. Tracking landslide displacements by multi-temporal DTMs: A combined aerial stereophotogrammetric and LIDAR approach in western Belgium. – Engineering Geol. **99**(1–2): 11–22.

Dupriez, G. L. & Demarée, G. R. (1989): Contribution à l'étude des relations intensité-durée-fréquence des précipitations. Totaux pluviométriques sur des périodes continues de 1 à 30 jours. II. – Analyse des séries pluviométriques d'au moins 30 ans. Miscellanea Série A, 9. IRM–KMI, 53 pp.

Fiorillo, F. (2003): Geological features and landslide mechanisms of an unstable coastal slope (Petacciato, Italy). – Engin. Geol. **67**(3–4): 255–267.

Gentili, G., Giusti, E. & Pizzaferri, G. (2002): Photogrammetric techniques for the investigation of the Cornoglio landslide. – In: Allison, R. J. (Ed.): Applied geomorphology: theory and practice: 39–48; Wiley, Chichester.

Glade, T. (2003): Landslide occurrence as a response to land use change: a review of evidence from New Zealand. – Catena **51**(3–4): 297–314.

Gullentops, F., Bogemans, F., De Moor, G., Paulissen, E. & Pissart, A. (2001): Quaternary lithostratigraphic units (Belgium). – Geol. Belgica **4**(1–2): 153–164.

Guthrie, R. H. (2002): The effects of logging on frequency and distribution of landslides in three watersheds on Vancouver Island, British Columbia. – Geomorphol. **43**(3–4): 273–292.

Hapke, C. J. (2005): Estimation of regional material yield from coastal landslides based on historical digital terrain modelling. – Earth Surf. Proc. and Landf. **30**(6): 679–697.

IRM – KMI (2005): Daily rainfall from 1951 until 2004, station 1402, Oudenaarde. Royal Meterorological Institute of Belgium.

Jacobs, P., De Ceukelaire, M., De Breuck, W. & De Moor, G. (1999): Toelichtingen bij de geologische kaart van België – Wlaams Gewest, Kaartblad (29) Kortrijk 1:50,000. Ministerie van Economische Zaken and Ministerie van de Vlaamse Gemeenschap, 68 pp.

Jakob, M. (2000): The impacts of logging on landslide activity at Clayoquot Sound, British Columbia. – Catena **38**(4): 279–300.

Jibson, R. W., Harp, E. L. & Michael, J. A. (2000): A method for producing digital probabilistic seismic landslide hazard maps. – Engin. Geol. **58**(3–4): 271–289.

Kääb, A. (2002): Monitoring high-mountain terrain deformation from repeated air- and spaceborne optical data: examples using digital aerial imagery and ASTER data. – ISPRS J. of Photogrammetry and Remote Sensing **57**(1–2): 39–52.

Keaton, J. R. & DeGraff, J. V. (1996): Surface observation and geologic mapping. – In: Turner, A. K. & Schuster, R. L. (Eds.): Landslides: investigation and mitigation. Transportation Research Board, Special Report 247, National Research Council. National Academy Press, Washington D. C., pp. 178–230.

Keefer, D. K. (1984): Landslides caused by earthquakes. – Geol. Soc. of Amer. Bull. **95**(4): 406–421.

Lantuit, H. & Pollard, W. H. (2005): Temporal stereophotogrammetric analysis of retrogressive thaw slumps on Herschel Island, Yukon territory. – Natural Hazards and Earth System Sciences **5**(3): 413–423.

Lourenço, S. D. N., Sassa, K. & Fukuoka, H. (2006): Failure process and hydrologic response of a two layer physical model: implications for rainfall-induced landslides. – Geomorphology **73**(1–2): 115–130.

Mikhail, E. M., Bethel, J. S. & McGlone, J. C. (2001): Introduction to modern photogrammetry. – Wiley, New York, 479 pp.

Montgomery, D. R., Schmidt, K. M., Greenberg, H. M. & Dietrich, W. E. (2000): Forest clearing and regional landsliding. – Geology **28**(4): 311–314.

Nyssen, J., Moeyersons, J., Poesen, J., Deckers, J. & Haile, M. (2003): The environmental significance of the remobilisation of ancient mass movements in the Atbara-Tekeze headwaters, Northern Ethiopia. – Geomorphology **49**(3–4): 303–322.

Oka, N. (1998): Application of photogrammetry to the field observation of failed slopes. Engineering Geology **50**(1–2): 85–100.

Ost, L., Van Den Eeckhaut, M., Poesen, J. & Vanmaercke-Gottigny, M. C. (2003): Characteristics and spatial distribution of large landslides in the Flemish Ardennes (Belgium). – Z. Geomorph. N. F. **47**(3): 329–350.

Parise, M. & Wasowski, J. (1999): Landslide activity maps for landslide hazard evaluation: three case studies from southern Italy. – Natural Hazards **20**(2–3): 159–183.

Polemio, M. & Sdao, F. (1999): The role of rainfall in the landslide hazard: the case of the Avigliano urban area (Southern Apennines, Italy). – Engineering Geol. **53**(3–4): 297–309.

Refice, A. & Capolongo, D. (2002): Probabilistic modeling of uncertainties in earthquake-induced landslide hazard assessment. – Computers & Geosciences **28**(6): 735–749.

Schmidt, K. M., Roering, J. J., Stock, J. D., Dietrich, W. E., Montgomery, D. R. & Schaub, T. (2001): The variability of root cohesion as an influence on shallow landslide susceptibility in the Oregon Coast Range. – Canad. Geotechn. J. **38**(5): 995–1024.

Sidle, R. C., Ziegler, A. D., Negishi, J. N., Nik, A. R., Siew, R. & Turkelboom, F. (2006): Erosion processes in steep terrain – Truths, myths, and uncertainties related to forest management in Southeast Asia. – Forest Ecol. and Managem. **224**(1–2): 199–225.

Stefanini, M. C. (2004): Spatio-temporal analysis of a complex landslide in the Northern Apennines (Italy) by means of dendrochronology. – Geomorphology **63**(3–4): 191–202.

Uchida, T., Kosugi, K. & Mizuyama, T. (2001): Effects of pipeflow on hydrological process and its relation to landslide: a review of pipeflow studies in forested headwater catchments. – Hydrol. Processes **15**(11): 2151–2174.

Van Den Eeckhaut, M. (2006): Spatial and temporal patterns of landslide in hilly regions. The Flemish Ardennes (Belgium), Katholieke Universiteit Leuven, Leuven, 250 pp.

Van Den Eeckhaut, M., Muys, B., Van Loy, K., Poesen, J. & Beeckman, H. (accepted): Evidence for repeated re-activation of old landslides under forest. – Earth Surface Proc. and Landf.

Van Den Eeckhaut, M., Poesen, J., Dewitte, O., Demoulin, A., De Bo, H. & Vanmaercke-Gottigny, M. C. (2007a): Reactivation of old landslides: lessons learned from a case-study in the Flemish Ardennes (Belgium). – Soil Use and Management **23**(2): 200–211.

Van Den Eeckhaut, M., Poesen, J., Verstraeten, G., Vanacker, V., Moeyersons, J., Nyssen, J. & van Beek, L. P. H. (2005): The effectiveness of hillshade maps and expert knowledge in mapping old deep-seated landslides. – Geomorphology **67**(3–4): 351–363.

Van Den Eeckhaut, M., Poesen, J., Verstraeten, G., Vanacker, V., Nyssen, J., Moeyersons, J., van Beek, L. P. H. & Vandekerckhove, L. (2007b): Use of LIDAR-derived images for mapping old landslides under forest. – Earth Surface Proc. and Landf. **32**(5): 754–769.

Van Den Eeckhaut, M., Verstraeten, G. & Poesen, J. (2007c): Morphology and internal structure of a dormant landslide in a hilly area: The Collinabos landslide (Belgium). – Geomorphology **89**(3–4): 258–273.

van Westen, C. J. & Getahun, F. L. (2003): Analyzing the evolution of the Tessina landslide using aerial photographs and digital elevation models. – Geomorphology **54**(1–2): 77–89.

Vanmaercke-Gottigny, M. C. (1980): Landslides as a morphogenetic phenomenon in a hilly region of Flanders (Belgium). – In: De Boodt, M. & Gabriels, D. (Eds.): Assessment of erosion. Wiley, Chichester, pp. 475–484.

Verstraeten, W. W., Muys, B., Feyen, J., Veroustraete, F., Minnaert, M., Meiresonne, L. & De Schrijver, A. (2005): Comparative analysis of the actual evapotranspiration of Flemish forest and cropland, using the soil water balance model WAVE. – Hydrology and Earth System Sciences **9**(3): 225–241.

Wasowski, J. (1998): Understanding rainfall-landslide relationships in man-modified environments: a case-history from Caramanico Terme, Italy. – Environmental Geol. **35**(2–3): 197–209.

Weber, D. & Herrmann, A. (2000): Contribution de la photogrammétrie numérique à l'étude spatio-temporelle de versants instables: l'exemple du glissement de Super-Sauze (Alpes-de-Haute-Provence). – Bull. de la Société géologique de France **171**(6): 637–648.

Addresses of the authors: Dr. Olivier Dewitte (Corresp. author), Department of Geography, Unit of Physical Geography and Quaternary, University of Liège, Allée du 6 Août 2, 4000 Liège, Belgium. E-Mail: odewitte@ulg.ac.be – Dr. Miet Van Den Eeckhaut, Physical and Regional Geography Research Group, K. U. Leuven, Celestijnenlaan 200-E, 3001 Heverlee, Belgium and Post-doctoral fellowship, Fund for Scientific Research, Flanders, Belgium – Prof. Dr. Jean Poesen, Physical and Regional Geography Research Group, K. U. Leuven, Celestijnenlaan 200-E, 3001 Heverlee, Belgium – Dr. Alain Demoulin, Department of Geography, Unit of Physical Geography and Quaternary, University of Liège, Allée du 6 Août 2, 4000 Liège, Belgium and National Fund for Scientific Research, Belgium.